FIRESIDE CORROSION TESTING OF CANDIDATE SUPERHEATER TUBE ALLOYS, COATINGS, AND CLADDINGS - PHASE III

J. L. Blough
W. W. Seitz

Foster Wheeler Development Corporation
12 Peach Tree Hill Road
Livingston, NJ 07039

ABSTRACT

In Phase I of this project, laboratory experiments were performed on a variety of developmental and commercial tubing alloys and claddings by exposing them to fireside corrosion tests, at 620-730 degrees C that simulated existing and advanced cycle superheaters or reheaters in a coal-fired boiler. Phase II (in situ testing) has exposed samples of 347, RA85H, HR3C, RA253MA, Fe_3Al + 5Cr, 310 modified, NF 709, 690 clad, 671 clad, and 800HT for up to approximately 16,000 hours to the actual operating conditions of a 250-MW, coal-fired boiler. The samples were installed on air-cooled, retractable corrosion probes, installed in the reheater cavity, and controlled to the operating metal temperatures of an existing and advanced-cycle, coal-fired boiler. Samples of each alloy were exposed for 4483, 11,348, and 15,883 hours of operation. The results of the 15,883 hours exposure have been issued in an interim report.

Phase III of this program will expose a variety of developmental and commercial tubing to conditions prototypical of air heaters of advanced cycle power-producing utility plant. This paper will summarize the proposed test conditions for the alloys to be tested.

INTRODUCTION

High-temperature fireside metal wastage in conventional coal-fired steam generators can be caused by gas-phase oxidation or liquid-phase coal-ash corrosion. Gas-phase oxidation is usually not a problem if tube and support materials are selected for their resistance to oxidation at the operating temperatures and for spalling, flaking, or other reactions to their environment. Coal-ash corrosion, on the other hand, usually results in accelerated attack and rapid metal wastage**C**even of stainless steels. The cause of this type of corrosion is usually the formation of alkali-iron-trisulfates on the tube surfaces. Some investigators have found that the presence of the low-melting-point alkali-aluminum sulfates also causes this type of corrosion. The corrosion occurs at the gas/ash interface where liquid sulfates actively corrode the surface of the metal beneath an overlying ash deposit[2-5]. In an air heater application the tubes will also be exposed to much higher temperatures approaching 2000 degrees F where the alkali sulfate corrosion mechanism is operative.

While substantial progress has been achieved through laboratory testing, actual utility service exposures are evidently necessary to verify any conclusions drawn from these tests. A number of important environmental parameters cannot be fully simulated in the laboratory[6-7].

- The actual composition of the deposits formed on the tubes is more complex than the composition of the simulated ash.
- The SO_3, formed by heterogeneous reaction on cooled surfaces, is variable.
- Very large temperature gradients occur within the ash deposits.
- The ash and fuel gas move past tubes at high velocity; the rate varies with design.
- The composition of the corrosive deposits changes with time.
- Metal and flue gas temperatures fluctuate.
- Fly-ash erosion removes the protective oxides, exposing a clean surface to fresh ash.

Foster Wheeler Development Corporation (FWDC) has performed a number of literature reviews and recent updates discussing the variables affecting the mechanism[6-8] of coal-ash corrosion. Additionally, Foster Wheeler has conducted two sizable research projects—one a laboratory and in situ field testing at three utilities of commercially available alloys[6,10,13-15] and this program (ORNL-FW2), combining laboratory and field testing to more completely cover the controlling variables for a longer duration[11].

PHASE I RESULTS

In Phase I of this ORNL program, "Fireside Corrosion Testing of Candidate Superheater Tube Alloys, Coatings, and Claddings," 20 commercial and developmental alloys were evaluated[10]. The coupons of the metals were exposed to multiple types of synthetic coal ash and synthetic flue gases at 650 and 700°C (1202 and 1292°F) for up to 800 hours.

Chromium content was found to be the largest factor in determining the resistance of an alloy to liquid coal-ash corrosion. For stainless steels and nickel alloys, additions of chromium up to 25 percent provided increased resistance to coal-ash attack; however, above the 25-percent chromium level, there appeared to be minimal benefit from more chromium, possibly because of the higher nickel content of those alloys.

Molybdenum, on the other hand, may be detrimental to corrosion resistance. Silicon and aluminum were also beneficial, but to a lesser extent. The iron-aluminide intermetallics also showed a chromium dependence. Aluminides containing 5-percent chromium performed markedly better overall than those containing 2-percent chromium. The more resistant alloys showed lower corrosion rates at longer exposure times, indicating the formation of a passive layer; the less-resistant alloys exhibited increasing corrosion rates at longer exposures. Lower-chromium alloys generally suffered greater wastage rates at the higher testing temperature [700°C (1292°F)], while higher-chromium alloys suffered the same amount of wastage at 650 (1202) as at 700°C (1292°F).

Both the alkali content in the ash and SO_2 concentration in the flue gas affect the corrosivity of the alkali-iron-trisulfates in the ash layer. An increase in either resulted in a more corrosive environment and higher wastage rates.

PHASE II CORROSION PROBE TEST PLAN

In this project, the field tests comprised corrosion probe testing, coal characterization, and deposit/corrosion product analysis. The coals were analyzed to provide fuel characterization, a deposit analysis data bank, and possibly a corrosivity index for predicting corrosivity under various combustion conditions. The equipment and the procedures for this phase have been previously used and perfected at three different utilities for over 3 years of in situ testing at each station.

The utility that acts as host for test exposures should be burning an aggressive fuel to adequately evaluate the candidate alloys. The coals being burned at Tennessee Valley Authority's (TVA's) Gallatin Station had been previously analyzed, and numerous corrosion indices predicted high corrosivity in addition to the fact that installed T22 and Type 304SS tubing experienced about 7 years of life in the superheaters and reheaters of units 1 and 2.

SELECTION OF MATERIALS FOR CORROSION PROBES

FWDC laboratory tested 20 different materials[11]. Because this quantity was impractical from both an economic and a probe-length standpoint, fewer materials (the ten listed in Table 1) were selected for the field tests. These materials provided a range of compositions and cost for both the commercially available and developmental alloys and claddings.

Table 1. Chemical Composition of Candidate Alloys (%)

Alloy	Cr	Ni	Others
85 H	18	15	Al = 1, Si = 3.9
Type 347	17-19	9-13	(Nb + Ta) = 10 × C (min.)
NF 709	20	25	Mo = 1.5, Mn = 1.0, Si = 0.6
253 MA	21	11	Si = 1.7
HR3C	25	20	Nb = 0.4
671 Clad/LSS*	48	52	
690 Clad/LSS*	30	58	
Fe_3Al + 5Cr	5	---	Al = 17
310 Modified	25	20	Ta = 1.5
800HT	21	32	Al + Ti = 1

*LSS - 14Cr, 17Ni, 2.25Mo, V, Ti, Nb, N

FIELD CORROSION PROBE DESIGN

The corrosion probes were designed to provide realistic exposures of metal samples to both actual boiler environments and also at the higher anticipated metal temperatures of an advanced plant. The operation of the probes is independent from the main boiler, allowing removal without a boiler outage, and a fail-safe design that removes the probe from the boiler if there are any malfunctions. With these features, years of testing will not be compromised by a sudden overheating of the system.

The probes were exposed for 4483, 11,348, and 15,883 hours. Ring samples [38.1 mm (1.5 in.) wide] of the candidate alloys listed in Table 2 were installed at the end of the 2.56-m-long probe. The probe was cooled by air that flowed in the annular region between the probe tube ID and the inner tube OD. The tapered inner tube was designed to obtain two bands of temperature on the outer surface of the samples. The alloy samples were duplicated in such a manner as to expose each alloy to a temperature in each of the temperature bands [621 to 677°C (1150 to 1250°F) and 677 to 727°C (1250 to 1340°F)].

The control system monitored the selected control thermocouple and modulated the airflow to maintain an average surface metal temperature for each temperature band. The probes retracted automatically if failure of the cooling-air supply system or any other malfunction (instrument signal, power failure, or computer failure) caused the probe temperature to exceed the set limit of 746°C (1375°F) for 2 minutes. The number of hours in various temperature bands were counted, and the weighted average temperature over the complete test period was then obtained. Once the effective temperature was obtained for the ends of each test section, the effective temperature for each alloy sample was calculated from the temperatures at the end points of the test section and the thermal properties of each alloy.

The locations in this plant were chosen because of cavity access and because they best represented the locations for the reheater or superheater outlet on the "Advanced Cycle" unit.

In an ideal coal-ash corrosion probe exposure, only one coal would be burned at the plant. The practice of burning one coal is not common at many utilities since most have multiple long-term coal contracts; in fact, many are buying coal on the spot market. Gallatin burns a number of eastern high-sulfur coals, mainly Island Creek, Warrior, Dotiri, Pattiki, and Constain, which are known to be corrosive and prone to alkali-iron-trisulfate

formation. The Borio Index[16] for these coals typically ranges from 2.0 to 4.1, and the chloride level is 450 to 3000 ppm.

POST-EXPOSURE ANALYSIS

At the end of each test period, the designated probe was removed, and post-exposure metallurgical evaluation was performed. The laboratory analysis of the removed deposits characterized the composition and determined whether alkali sulfates were present and aided in interpreting the effects of fuel changes on coal-ash corrosion.

MACROSCOPIC EXAMINATION

Both the 11,348- and 15,883-hour probes were received with a tan deposit on their outer surfaces. The deposits were removed and stored separately for later examination. Two 1/4-in.-long transverse ring sections were removed from each sample on both probes. One of the ring sections was lightly grit blasted and used for thickness measurements while the other was mounted for microscopic and SEM/EDX analysis.

Shallow pitting and some surface roughening are evident in some of the samples. The more prominent surface roughness or pitting was noted on samples 1 (RA85H), 2 (347), 3 (NF 709), 11 (RA85H), and 12 (347) from the 11,348-hour probe, and 1 (RA85H), 2 (347), 4 (253MA), 11 (RA85H) and 12 (347) in the 15,883-hour probe. Post-exposure wall thickness readings were performed at the 45-, 135-, and 270-degree locations, and calculated wall loss at the three locations. [Note: Further microexamination revealed that some of the wall loss in composite tube samples 6, 7, 16, and 17 resulted from the oxidation of the lower alloy LSS inside surface and not from corrosion of the higher alloy outside surface. One half of the scale thickness was calculated to be metal loss and was therefore added back into the wall thickness measurements to determine the loss from the OD only. Also, because of the swelling of the Fe_3Al samples, possibly because of a phase change, wall thickness losses were negative and could not be used to indicate wall loss as a result of corrosion. Since the corrosion was minimal and the original surfaces could be determined, the wall thickness loss was measured microscopically.]

MICROSCOPIC EXAMINATION and EDX ANALYSIS

All the specimens from each probe were mounted and microscopically examined to determine the subsurface penetration. Short sections from the 45-, 135-, and 270-degree locations of the samples were prepared for microscopic examination, and the depth of penetration was measured for all the samples.

DISCUSSION

The examination revealed that, for the most part, the 15,883-hour probe samples exhibited the most attack with respect to the microscopic appearance and total metal wastage of the samples. In terms of the corrosion rate, if the short-term probe is discounted, then for the most part, the 15,883-hour probe has a higher rate when extrapolated linearly. None of the samples were immune to the environment; all exhibited varying degrees of internal oxidation, while most displayed evidence of carburization and sulfidation. The total metal wastage and corrosion rate values are given in Table 4.

The relationship between the corrosion resistance and material chemistry appears to follow trends established in earlier work. Chromium content was found to be the largest factor in determining the resistance of an alloy to liquid coal-ash corrosion. For stainless steels and nickel alloys, additions of chromium between 20 and 25 percent provide increased resistance to coal-ash attack; however, above the 25-percent chromium level, there appears to be minimal benefit from more chromium, possibly because of the higher nickel content of those higher-chromium-containing alloys. This was confirmed based on the collected data which clearly illustrate the corrosion resistance improving when the chromium content exceeds the 20-percent mark. Consequently, with the exception of the iron-aluminide alloy, the higher-chromium-containing alloys displayed very promising corrosion rates (#10 mils/yr).

It was determined that the benefits of nickel addition reached their limit at about 35 percent by comparing 800H to 690. Above this amount, an increase in nickel seemed not to produce any additional benefits except if about 50-percent chromium was added (671). Silicon and aluminum were also beneficial, but to a lesser extent.

The iron-aluminide intermetallics also showed a chromium dependence in the phase 1 testing. Aluminides containing 5-percent chromium performed markedly better overall than those containing 2-percent chromium. In the phase 2 field test, only the 5-percent chromium aluminide was used.

Closer examination of the other elements employed as alloying additions revealed some interesting results. The materials that contained aluminum gave results at each position of the performance scale. The Fe_3Al contained 17-percent aluminum and only 5-percent chromium; however, it exhibited a low-end total metal wastage and corrosion rate at both hot and cool temperature locations, in both the 11,348- and 15,883-hour probes. The noticeable trait that separated it from the other alloys was that it had an aluminum-rich scale as well as an aluminum-rich phase throughout its matrix. In this case, the aluminum scale seemed to be inert and sufficiently stable to prevent the ingress of any aggressive species. The RA85H and the 800HT materials also contained aluminum in the 1-percent range. The difference between the two was that the RA85H contained silicon (3.9 percent) while the 800HT contained titanium (<1 percent). The 800HT gave very consistent performance (about 3 to 4 mils/yr) and was ranked in the middle of the group (around fourth or fifth best). On the other hand, the corrosion behavior of RA85H was very erratic, exhibiting higher wastage values in the 11,348-hour samples and the hotter 15,883-hour sample but low values in the cooler 15,883-hour sample. The results suggest that the aluminum in higher concentrations seemed to have a more profound effect on imparting resistance to corrosion, which agrees with the results achieved by Rehn[8].

The benefits of silicon as an alloying addition were also examined because of the potential for forming a protective subscale of silica. Of the three silicon-containing materials, RA253MA (1.7 percent) exhibited the best corrosion resistance in the higher temperature ranges followed by NF 709 (0.6 percent) and RA85H (3.9 percent). In the cooler temperature range on the 11,348-hour probe, the RA85H material exhibited the best resistance, while the RA253MA displayed the worst. The results are not conclusive concerning any beneficial effects of silicon additions because the results were different in the two different temperature ranges. However, one could postulate that in the lower temperature range, both the silicon and aluminum content helped to stabilize the protective scale on RA85H, while in the higher temperature range, the higher chromium content in the RA253MA, along with the addition of the silicon, provided a more protective scale.

The more resistant alloys showed lower corrosion rates at longer exposure times, indicating the formation of a protective layer; the less-resistant alloys exhibited increasing corrosion rates at longer exposures (Figures 1 and 2). Also, the lower-chromium alloys generally suffered greater wastage rates at the higher testing temperature [700EC (1292EF)], whereas higher-chromium alloys suffered similar levels of wastage at 650 (1202) as at 700EC (1292EF).

The temperature-dependence relationship of coal-ash corrosion is defined by a bell-shaped curve due to the thermodynamic stability of the alkali-iron-trisulfate[2,3,4]. Typically, it has been observed that the wastage increases as the temperature rises in the temperature range where the molten alkali-iron-trisulfate (1112 to 1292°F) is stable. The decrease in wastage in the higher temperature range is due to the fact that the molten alkali-iron-trisulfate disassociates. The peak temperature for wastage is somewhat different for each alloy, since the temperature range in which the molten salt is stable depends on the interaction of the molten salt with the surface of the alloy. Corrosion products generated by the test materials can also have an effect on the melting temperature of the salt. The corrosion rates of the 11,348- and 15,883-hour samples were plotted against their respective temperature ranges to examine the temperature dependency displayed by the materials. Even though the examination revealed no clear temperature dependency with 15,883-hour samples, most of the materials in the 11,348-hour group exhibited a trend to decreased corrosion rate with increased temperature. Plotting the two temperature ranges separately against the three exposure times revealed a general trend for the corrosion rate to be essentially constant or to slightly increase with time, with some exceptions. For the most part, the 15,883-hour samples exhibited a higher corrosion rate than their 4000- or 11,348-hour counterparts.

Table 4. Results of Numerical Evaluation

Sample	Cr (%)	Ni (%)	Total Metal Wastage (mils)			Corrosion Rate (mils/yr)			Temperature (°F)		
			4483 (hr)	11,348 (hr)	15,883 (hr)	4483 (hr)	11,348 (hr)	15,883 (hr)	4483 (hr)	11,348 (hr)	15,883 (hr)
Fe_3Al	5	0	0.0	4.0	5.0	0.0	3.1	2.8	1313	1307	1319
Fe_3Al	5	0	0.0	5.5	6.5	0.0	4.2	3.6	1223	1231	1229
RA85H	18	12	2.5	5.0	12.5	4.9	3.9	6.9	1260	1266	1267
RA85H	18	12	3.0	9.6	4.2	5.9	7.4	2.3	1157	1163	1156
347	18	15	2.7	5.7	21.6	5.3	4.4	11.9	1267	1272	1275
347	18	15	2.0	5.4	10.3	3.9	4.2	5.7	1166	1172	1167
NF 709	20	25	0.5	2.5	10.7	1.0	1.9	5.9	1275	1278	1282
NF 709	20	25	1.6	8.3	9.6	3.1	6.4	5.3	1176	1182	1177
RA253MA	21	11	2.4	2.4	5.6	4.7	1.9	3.1	1283	1284	1289
RA253MA	21	11	1.4	2.7	11.5	2.7	2.1	6.3	1185	1192	1187
800HT	21	32	1.5	3.1	7.6	2.9	2.4	4.2	1328	1319	1334
800HT	21	32	1.5	4.3	8.5	2.9	3.3	4.7	1242	1250	1250
310 Mod	25	20	0.0	4.1	7.2	0.0	3.2	4.0	1321	1313	1326
310 Mod	25	20	0.1	3.2	4.3	0.2	2.5	2.4	1233	1241	1239
HR3C	25	20	0.3	3.5	0.9	0.6	2.7	0.5	1290	1290	1297
HR3C	25	20	0.8	6.0	6.6	1.6	5.0	3.6	1195	1202	1198
690	30	58	0.5	3.0	7.9	1.0	2.3	4.4	1305	1301	1312
690	30	58	0.5	4.0	7.0	1.0	3.1	3.9	1214	1221	1219
671	48	52	0.5	3.5	5.0	1.0	2.7	2.8	1298	1295	1304
671	48	52	0.5	2.5	5.3	1.0	1.9	2.9	1204	1211	1208

PHASE II CONCLUSIONS

Based on the examination of the samples reported above, the following conclusions can be drawn:

- The effect of chromium was found to be beneficial up to 20 to 25 percent, with little further improvement at higher levels.
- Nickel was observed to have a beneficial effect up to about 35 percent, but higher levels did not reduce the corrosion and were sometimes detrimental, except if very high levels of chromium were added.
- The effect of aluminum was not clearly defined. At the lower percentages (≤1 percent), there was little observable effect on the ability to resist the molten trisulfate attack, but at higher concentrations, as in the Fe_3Al alloy (17-percent Al), where an alumina scale was formed, protective behavior was promoted.
- The effect of silicon on the corrosion resistance of the test materials could not be clearly determined because of the inconsistent results from the high- and low-temperature ranges of the 11,348- and 15,883-hour probes.
- The ranking of the alloys based on the longest exposure was as follows:

1146-1249EF		1267-1341EF	
Material	**Mils/yr**	**Material**	**Mils/yr**
85H	2.3	HR3C	0.5
310 Ta Modified	2.4	671	2.8
671	2.9	Fe_3Al	2.8
Fe_3Al	3.6	253MA	3.1
HR3C	3.6	310 Ta Modified	4.0
690	3.9	800HT	4.2
800HT	4.7	690	4.4
NF 709	5.3	NF 709	5.9
347	5.7	85H	6.9
253MA	6.3	347	11.9

PHASE III

This phase of the workscope will address the alkali sulfate and oxidation mechanisms that are operative at 1800 to 2000°F in an air heater-type application. A variety of developmental and commercial alloys, especially oxide dispersion-strengthened (ODS) alloys, will be exposed under conditions prototypical of air heaters of an advanced-cycle, power-producing utility plant. Six material samples will be part of an air-cooled, corrosion-testing probe inserted into the reheater of a 250-MW, coal-fired utility boiler. The samples will be exposed for 4000, 12,000 and 16,000 hours, after which they will be metallurgically examined to characterize the wastage mechanism.

Temperature probes were inserted in two locations at the utility boiler and monitored for one month of typical cyclic operation. The average temperature for the two locations was 1750 and 2250 respectively. The temperature at the higher temperature location is acceptable for the air-cooled corrosion probe.
Two access doors were found at the area measuring 2250 °F and designs were formulated for the corrosion probe attachment to the casing. The air lines and control panel used for Phase 2 have to be rerouted to the higher temperature location for Phase 3. Estimates for that work are being obtained and the work will begin shortly.

The tubing materials received for test were of multiple ID and OD dimensions therefore the computer program used to design the probe had to be modified. An adequate thermal design was reached and the corrosion probe design finalized. Alloy 230 was selected to be the alloy for comparison purposes. The probe fabrication drawings are being finalized and probe manufacture will begin shortly.

TOTAL WASTAGE vs. % CHROMIUM FOR 16,000 HOUR PROBE
(1146 - 1249 Deg F)

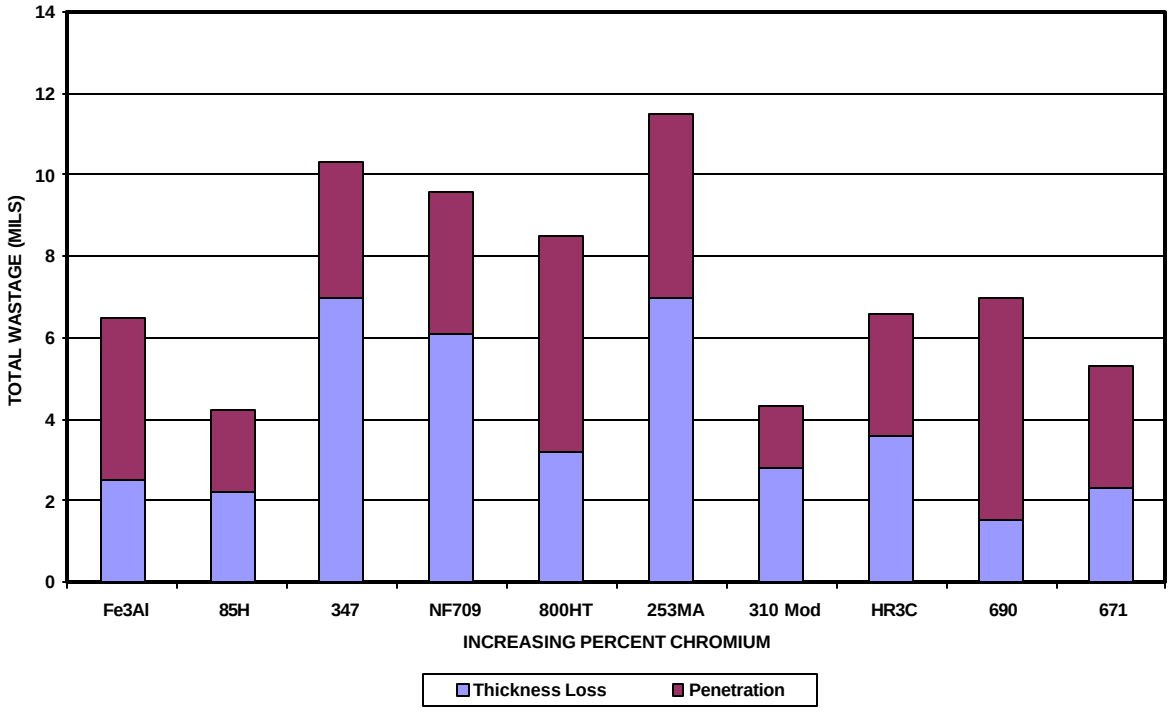

TOTAL WASTAGE vs. % CHROMIUM FOR 16,000 HOUR PROBE
(1267 - 1341 Deg F)

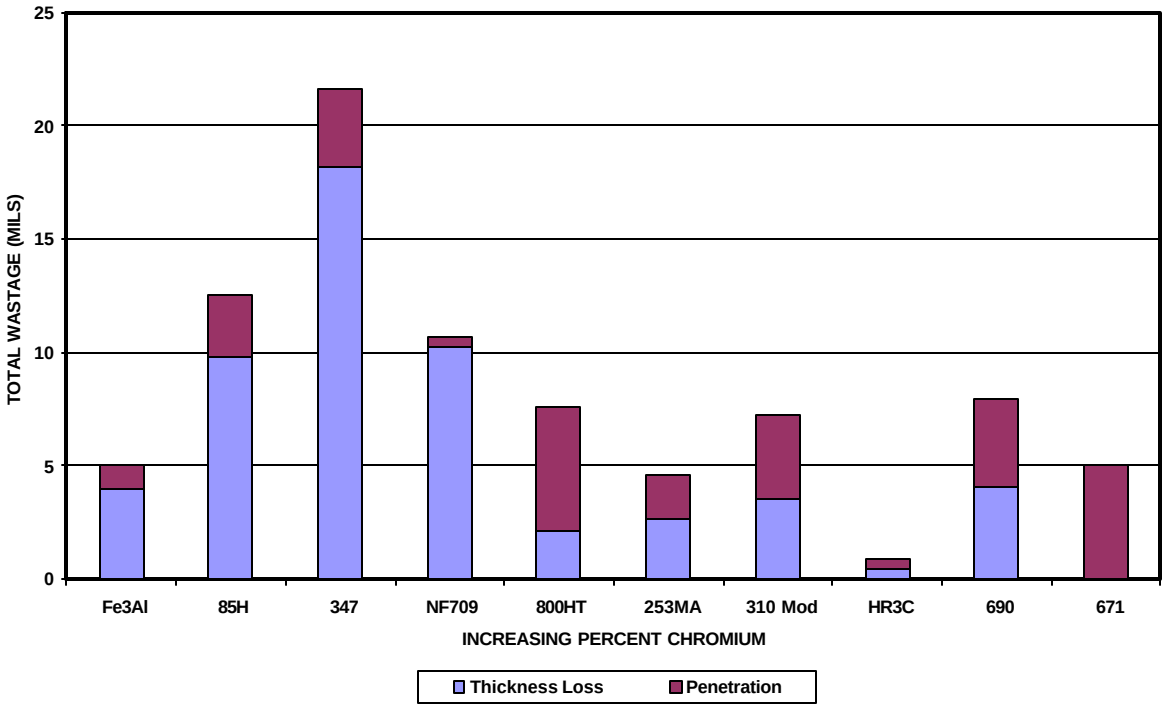

REFERENCES

1. J. L. Blough, "Fireside Corrosion, Testing of Candidate Superheater Tube Alloys, Coatings, and Claddings—Phase II Field Testing, Topical Report," Livingston, NJ: Foster Wheeler Development Corporation, August 1996. ORNL/SUB/93-SM401/01.

2. W. Nelson and C. Cain, Jr., "Corrosion of Superheaters and Reheaters of Pulverized-Coal-Fired Boilers," *Transactions of the ASME, Journal of Engineering for Power*, July 1960, pp. 194-204.

3. W. T. Reid, "Formation of Alkali Iron Trisulphates and Other Compounds Causing Corrosion in Boilers and Gas Turbines," Project Review July 1, 1966-June 30, 1968, prepared by Battelle Memorial Institute, Columbus, OH, June 1968.

4. W. T. Reid, *External Corrosion and Deposits: Boilers and Gas Turbines*, American Elsevier Publishing Company, New York, 1974.

5. G. J. Hills, "Corrosion of Metals by Molten Salts," *Proceedings of the Marchwood Conference: Mechanism of Corrosion by Fuel Impurities*, Johnson and Littler, eds., Butterworths, London, 1963.

6. J. L. Blough, G. J. Stanko, M. Krawchuk, W. Wolowodiuk, and W. Bakker, "In Situ Coal Ash Corrosion Testing for 2 Years at Three Utilities," International EPRI Conference on Improved Technology for Fossil Power Plants New and Retrofit Applications, Washington, DC, March 1-3, 1993.

7. S. Kihara, K. Nakagawa, A. Ohtomo, H. Aoki, and S. Ando, "Simulating Test Results for Fireside Corrosion of Superheater & Reheater Tubes Operating at Advanced Steam Conditions in Coal-Fired Boilers, *High Temperature Corrosion in Energy Systems*, TMS/AIME, M. F. Rothman, ed., 1984, pp. 361-376.

8. I. M. Rehn, "Fireside Corrosion of Superheater Alloys for Advanced Cycle Steam Plants," Palo Alto, CA: Electric Power Research Institute, 1987. EPRI 5195.

9. S. Van Weele and J. L. Blough, "Literature Search Update—Fireside Corrosion Testing of Candidate Superheater Tube Alloys, Coatings, and Claddings," Livingston, NJ: Foster Wheeler Development Corporation, September 1990. FWC/FWDC/TR-90-11.

10. W. Wolowodiuk, S. Kihara, and K. Nakagawa, "Laboratory Coal Ash Corrosion Tests," Palo Alto, CA: Electric Power Research Institute, July 1989. GS-6449.

11. S. Van Weele and J. L. Blough, "Fireside Corrosion Testing of Candidate Superheater, Tube Alloys, Coatings, and Claddings," Livingston, NJ: Foster Wheeler Development Corporation, August 1991. ORNL/SUB/89-SA187/02.

12. I. M. Rehn, "Fireside Corrosion of Superheater and Reheater Tubes," Palo Alto, CA: Electric Power Research Institute, 1980. CS-1653.

13. W. Wolowodiuk, et al., "Coal-Ash Corrosion Investigations," *Proceedings of the First International Conference on Improved Coal-Fired Power Plants.* Palo Alto, CA: Electric Power Research Institute, November 1986.

14. J. L. Blough, M. T. Krawchuk, G. J. Stanko, and W. Wolowodiuk, "Superheater Corrosion Field Test Results," Palo Alto, CA: Electric Power Research Institute, November 1993. TR-103438.

15. J. L. Blough and W. T. Bakker, "Measurement of Superheater Corrosion Caused by Molten Alkali Sulfates," First International Conference on Heat-Resistant Materials, to be presented at the ASM International, Lake Geneva, WI, September 22-26, 1991.

16. R. W. Borio and R. P. Hensel, "Coal-Ash Composition as Related to High-Temperature Fireside Corrosion and Sulfur-Oxides Emission Control," *Transactions of the ASME, Journal of Engineering for Power*, Vol. 94, 1972, pp. 142-148.